8-1-2020

Thermodynamics of Rotating Quantum Matter in the Virial Expansion

Casey E. Berger
College of Arts & Sciences, cberger@smith.edu

K. J. Morrell
College of Arts & Sciences

J. E. Drut
College of Arts & Sciences

Thermodynamics of rotating quantum matter in the virial expansion

C. E. Berger, [*] K. J. Morrell, and J. E. Drut
Department of Physics and Astronomy, University of North Carolina, Chapel Hill, North Carolina 27599, USA

(Received 18 May 2020; accepted 14 July 2020; published 6 August 2020)

We characterize the high-temperature thermodynamics of rotating bosons and fermions in two-dimensional (2D) and three-dimensional (3D) isotropic harmonic trapping potentials. We begin by calculating analytically the conventional virial coefficients b_n for all n in the noninteracting case, as functions of the trapping and rotational frequencies. We also report on the virial coefficients for the angular momentum and associated moment of inertia. Using the b_n coefficients, we analyze the deconfined limit (in which the angular frequency matches the trapping frequency) and derive explicitly the limiting form of the partition function, showing from the thermodynamic standpoint how both the 2D and 3D cases become effectively homogeneous 2D systems. To tackle the virial coefficients in the presence of weak interactions, we implement a coarse temporal lattice approximation and obtain virial coefficients up to third order.

DOI: 10.1103/PhysRevA.102.023309

I. INTRODUCTION

The exploration of the phases of matter in regimes governed by quantum mechanics, i.e., quantum matter, is now carried out with increasing accuracy and controllability in ultracold-atom experiments [1–3]. The ability to tune the interaction strength via Feshbach resonances [4], introduce imbalances such as mass and polarization [5], vary the number of internal degrees of freedom, and control the temperature and external trapping potential have led to a huge parameter space that experimentalists can realize and manipulate [6]. These have, in turn, enabled a large body of work that continues to grow both qualitatively and quantitatively toward elucidating the properties of quantum systems in extreme conditions as a function of internal as well as thermodynamic parameters.

Most notably, experiments already more than two decades old achieved the first realizations of atomic Bose-Einstein condensates [7,8] and, about a decade later, fermionic superfluids [9,10], and since then experimentalists have continued to probe these systems in the various ways mentioned above and more. In particular, for both bosonic and fermionic systems, experimentalists early on realized rotating condensates and observed vortices and vortex lattices [11–13], the latter widely regarded as the "smoking gun" for superfluidity. From the condensed-matter standpoint, the interest in rotating condensates is often associated with the realization of exotic strongly correlated states (such as those associated with the fractional quantum Hall effect; see, e.g., [14]). In those systems, the limit of large vortex number, i.e., large angular momentum, corresponds to the "deconfinement limit" in which the angular frequency matches the trapping frequency, and is of particular interest as it admits a simple description (in the case of weak interactions) in terms of Landau levels.

While there exists a considerable body of work on such rotating condensates (see, e.g., [14,15] for reviews), i.e., work addressing the ground-state and low-temperature phases, less is known about the specifics of the high-temperature behavior of these systems. In particular, little is known about the quantum-classical crossover and how strong correlations (which play a crucial role in determining the shape of the phase diagram [16]) affect the normal phase of rotating strongly coupled matter.

In this work, we provide another piece of the puzzle by analyzing the high-temperature thermodynamics of rotating Bose and Fermi gases in two dimensions (2D) and 3D. To that end, we use the virial expansion and implement a coarse temporal lattice approximation recently put forward in Refs. [17–19]. The approximation allows us to bypass the requirement of solving the n-body problem to access the nth-order virial coefficient, which will be essential to address the effects of interactions. For the sake of simplicity, we focus on systems with two particle species with a contact interaction across species (i.e., no intraspecies interaction). These are routinely realized experimentally with ultracold atoms, both fermionic and bosonic. (Note that cases with intraspecies interactions are also possible, but independently tuning inter- and intraspecies interactions in experiments may pose a challenge.) Along the way, we present in detail several results for noninteracting systems which, while easy to obtain and should be textbook material, do not appear in the literature to the best of our knowledge. For both the interacting and noninteracting cases, we show results for the angular momentum and moment of inertia, as a function of temperature and rotation frequency, which can be experimentally tested.

Previous work addressing the high-temperature thermodynamics of rotating quantum gases, e.g., in interacting [20–23] as well as noninteracting [24,25] regimes, presents different analyses which are complementary to the present work. For instance, Refs. [20,21] address the thermodynamics of trapped rotating fermions using few-body solutions to obtain virial coefficients up to third order, but they only display the

[*]Present address: Department of Physics, Boston University, Boston, MA 02215, USA.

leading trapping frequency dependence of the results (which include energy and entropy, but not angular momentum or moment of inertia). On the other hand, Ref. [22] focuses on the effective theory for the lowest Landau level for a single species of bosons with intraspecies interactions (which is a different system and regime from the one considered here). Finally, Refs. [24,25] analyze the thermodynamics of rotating fermions, but do not report explicit results for virial coefficients.

II. HAMILTONIAN AND FORMALISM

As our focus is on systems with short-range interactions, such as dilute atomic gases or dilute neutron matter, the Hamiltonian reads

$$\hat{H} = \hat{H}_0 + \hat{V}_{\rm int}, \tag{1}$$

where

$$\hat{H}_0 = \hat{T} + \hat{V}_{\rm ext} - \omega_z \hat{L}_z, \tag{2}$$

and

$$\hat{T} = \sum_{s=1,2} \int d^d x\, \hat{\psi}_s^\dagger(\mathbf{x}) \left(-\frac{\hbar^2 \nabla^2}{2m} \right) \hat{\psi}_s(\mathbf{x}) \tag{3}$$

is the kinetic energy,

$$\hat{V}_{\rm ext} = \frac{1}{2} m \omega_{\rm tr}^2 \int d^d x\, \mathbf{x}^2 \left[\hat{n}_1(\mathbf{x}) + \hat{n}_2(\mathbf{x}) \right] \tag{4}$$

is the spherically symmetric external trapping potential,

$$\hat{V}_{\rm int} = -g_d \int d^d x\, \hat{n}_1(\mathbf{x}) \hat{n}_2(\mathbf{x}) \tag{5}$$

is the interaction, and

$$\hat{L}_z = -i \sum_{s=1,2} \int d^d x\, \hat{\psi}_s^\dagger(\mathbf{x}) (x \partial_y - y \partial_x) \hat{\psi}_s(\mathbf{x}) \tag{6}$$

is the angular momentum operator in the z direction. In polar or spherical coordinates, the differential operator in the above second-quantized form becomes simply $-i\partial/\partial\phi$, where ϕ is the azimuthal angle. In the above equations, the field operators $\hat{\psi}_s$, $\hat{\psi}_s^\dagger$ correspond to particles of species $s = 1, 2$, and $\hat{n}_s(\mathbf{x})$ are the coordinate-space densities. In the remainder of this work, we will take $\hbar = k_{\rm B} = m = 1$.

A. Thermodynamics and the virial expansion

The equilibrium thermodynamics of our quantum many-body system is captured by the grand-canonical partition function, namely,

$$\mathcal{Z} = {\rm tr}\left[e^{-\beta(\hat{H} - \mu \hat{N})} \right] = e^{-\beta \Omega}, \tag{7}$$

where β is the inverse temperature, Ω is the grand thermodynamic potential, $\hat{N}$ is the total particle number operator, and μ is the chemical potential for both species.

At this point, it is useful to review the parameters that control our system, including the thermodynamic ones; they are β, μ, $\omega_{\rm tr}$, ω_z, and g_d. We may then form dimensionless parameters, which we may choose to be $\beta\mu$, $\beta\omega_{\rm tr}$, $\beta\omega_z$, and λ, where the latter will typically involve a scattering length and will depend on whether we are examining the 2D or 3D problems (see below).

As the calculation of $\mathcal{Z}$ is a formidable problem in the presence of interactions, we resort to approximations and numerical evaluations in order to access the thermodynamics. To that end, in this work we will explore the virial expansion (see Ref. [26] for a review; see, also, [27]), which is an expansion around the dilute limit $z \to 0$, where $z = e^{\beta\mu}$ is the fugacity, i.e., it is a low-fugacity expansion. The coefficients accompanying the powers of z in the expansion Ω are the virial coefficients b_n,

$$-\beta\Omega = \ln \mathcal{Z} = Q_1 \sum_{n=1}^{\infty} b_n z^n, \tag{8}$$

where Q_1 is the one-body partition function. Using the fact that $\mathcal{Z}$ is itself a sum over canonical partition functions Q_N of all possible particle numbers N, namely,

$$\mathcal{Z} = \sum_{N=0}^{\infty} z^N Q_N, \tag{9}$$

we obtain expressions for the virial coefficients,

$$b_1 = 1, \tag{10}$$

$$b_2 = \frac{Q_2}{Q_1} - \frac{Q_1}{2!}, \tag{11}$$

$$b_3 = \frac{Q_3}{Q_1} - b_2 Q_1 - \frac{Q_1^2}{3!}, \tag{12}$$

and so on. In this work, we will not pursue the virial expansion beyond b_3. The Q_N can be written in terms of the partition functions $Q_{a,b}$ for a particles of type 1 and b particles of type 2,

$$Q_1 = 2Q_{1,0}, \tag{13}$$

$$Q_2 = 2Q_{2,0} + Q_{1,1}, \tag{14}$$

$$Q_3 = 2Q_{3,0} + 2Q_{2,1}, \tag{15}$$

and so on for higher orders. In the absence of intraspecies interactions, only the $Q_{1,1}$ and $Q_{2,1}$ are affected, such that the change in b_2 and b_3 due to interactions is entirely given by

$$\Delta b_2 = \frac{\Delta Q_{1,1}}{Q_1}, \tag{16}$$

$$\Delta b_3 = \frac{2\Delta Q_{2,1}}{Q_1} - \Delta b_2 Q_1. \tag{17}$$

We will use these expressions to access the high-temperature thermodynamics of bosons and fermions. To calculate $\Delta Q_{1,1}$ and $\Delta Q_{2,1}$, we will implement a coarse temporal lattice approximation, as described in the next section. Once we obtain the virial coefficients, we will rebuild the grand-canonical potential Ω to access the thermodynamics of the system as a function of the various parameters. In order to connect to the *physical* parameters of the systems at hand, one may use the value of Δb_2 as a renormalization condition by

relying on the exact answer [28], which is known at $\omega_z = 0$, namely,

$$\Delta b_2^{(2D)} = \frac{e^{-\beta\omega_{tr}}}{2}\sum_{n=0}^{\infty}\left[e^{-\beta\omega_{tr}2\nu_n(\lambda)} - e^{-\beta\omega_{tr}2n}\right], \quad (18)$$

$$\Delta b_2^{(3D)} = \frac{e^{-\beta\omega_{tr}3/2}}{2}\sum_{n=0}^{\infty}\left[e^{-\beta\omega_{tr}2\nu_n(\lambda)} - e^{-\beta\omega_{tr}2n}\right] \quad (19)$$

(see Ref. [29] for the 2D case and [30] for the 3D case), where $\omega_{tr}[2\nu_n(\lambda) + d/2]$ is the energy of the d-dimensional two-body problem in the center-of-mass frame. Using these expressions, one may fix the value of the dimensionless coupling for each system, for a given $\beta\omega_{tr}$. The use of Δb_2 as a physical quantity to renormalize the coupling constant was advocated in Refs. [17–19].

B. Single-particle basis and single-particle partition function in 2D and 3D

In evaluating the results of the coarse temporal lattice approximation presented below, we will use the eigenstates of $\hat{H}_0$ in 2D and 3D, in polar and spherical coordinates, respectively. We therefore present them in detail here for future reference, along with the corresponding single-particle partition function.

1. Two spatial dimensions

In 2D, the single-particle eigenstates of $\hat{H}_0$ in 2D are given by (see the Appendix)

$$\langle \mathbf{x}|\mathbf{k}\rangle = \frac{1}{\sqrt{2\pi}}R_{km}(\rho)e^{-im\phi}, \quad (20)$$

where

$$R_{km}(\rho) = N_{km}^{(2D)}\omega_{tr}^{1/2}\, e^{-\rho^2/2}\rho^{|m|}L_k^{|m|}(\rho^2), \quad (21)$$

where $\rho = \omega_{tr}^{1/2}\, r$, and

$$N_{km}^{(2D)} = \sqrt{2}\sqrt{\frac{k!}{(k+|m|)!}}, \quad (22)$$

with $L_k^{|m|}$ the associated Laguerre functions. We have used polar coordinates r, ϕ, and a collective quantum number $\mathbf{k} = (k, m)$, with $k = 0, 1, \ldots$ and m can take any integer value. The corresponding energy is

$$E_{km} = \omega_{tr}(2k + |m| + 1) + \omega_z m. \quad (23)$$

With this spectrum, it is a simple matter to calculate Q_1, which by definition is

$$Q_1 = \sum_{\mathbf{k}} e^{-\beta E_{\mathbf{k}}}. \quad (24)$$

Thus, in 2D,

$$Q_1 = 2\sum_{k,m} e^{-\beta E_{km}} = \frac{2\, e^{-\beta\omega_{tr}}}{(1 - e^{-\beta\omega_+})(1 - e^{-\beta\omega_-})}, \quad (25)$$

where $\omega_\pm = \omega_{tr} \pm \omega_z$ and the overall factor of 2 reflects the fact that we have two particle species.

2. Three spatial dimensions

In 3D, the single-particle eigenstates of $\hat{H}_0$ in 3D are

$$\langle \mathbf{x}|\mathbf{k}\rangle = R_{kl}(\rho)P_l^m(\cos\theta)e^{-im\phi}, \quad (26)$$

where $P_l^m(x)$ are the associated Legendre functions and

$$R_{kl}(\rho) = N_{kl}^{(3D)}\omega_{tr}^{3/4}e^{-\rho^2/2}\rho^l L_k^{l+1/2}(\rho^2), \quad (27)$$

where

$$N_{kl}^{(3D)} = \sqrt{\frac{1}{\sqrt{4\pi}}\frac{2^{k+2l+3}\,k!}{(2k+2l+1)!!}}. \quad (28)$$

Here, we have used spherical coordinates r, θ, ϕ, where θ is the polar angle and ϕ is the azimuthal angle. The collective quantum number $\mathbf{k} = (k, l, m)$ is such that $k \geqslant 0$, $l \geqslant 0$, and $-l \leqslant m \leqslant l$. The corresponding energy is

$$E_{klm} = \omega_{tr}(2k + l + 3/2) + \omega_z m. \quad (29)$$

Here, the corresponding single-particle partition function is given by

$$Q_1 = \frac{2e^{-\beta\omega_{tr}3/2}}{(1 - e^{-\beta\omega_{tr}})(1 - e^{-\beta\omega_+})(1 - e^{-\beta\omega_-})}. \quad (30)$$

C. Coarse temporal lattice approximation

To calculate the interaction-induced change in the canonical partition functions $\Delta Q_{1,1}$ and $\Delta Q_{2,1}$, we propose an approximation which consists in keeping only the leading term in the Magnus expansion,

$$e^{-\beta(\hat{H}_0+\hat{V}_{int})} = e^{-\beta\hat{H}_0}e^{-\beta\hat{V}_{int}} \times e^{-\frac{\beta^2}{2}[\hat{H}_0,\hat{V}_{int}]} \times \cdots, \quad (31)$$

where the higher orders involve exponentials of nested commutators of $\hat{H}_0$ with $\hat{V}_{int}$. Thus, the leading order (LO) in this expansion consists in setting $[\hat{H}_0, \hat{V}_{int}] = 0$, which becomes exact in the limit where either $\hat{H}_0$ or $\hat{V}_{int}$ can be ignored (i.e., respectively, the strong- and weak-coupling limits). Previous explorations of this approximation, by us and others [17–19,28,31,32], indicate that LO-level results (the so-called semiclassical approximation) for trapped systems are not only qualitatively but also quantitatively correct at weak coupling.

1. Two-body contribution $\Delta Q_{1,1}$.

To calculate Δb_2, we will need the above result for Q_1, but also $\Delta Q_{1,1}$. At leading order in our coarse temporal lattice approximation,

$$\begin{aligned} Q_{1,1} &= \mathrm{tr}_{1,1}[e^{-\beta\hat{H}_0}e^{-\beta\hat{V}_{int}}] \\ &= \sum_{\mathbf{k}_1,\mathbf{k}_2,\mathbf{x}_1,\mathbf{x}_2} \langle \mathbf{k}_1\mathbf{k}_2|e^{-\beta\hat{H}_0}|\mathbf{x}_1\mathbf{x}_2\rangle\langle \mathbf{x}_1\mathbf{x}_2|e^{-\beta\hat{V}_{int}}|\mathbf{k}_1\mathbf{k}_2\rangle \\ &= \sum_{\mathbf{k}_1,\mathbf{k}_2,\mathbf{x}_1,\mathbf{x}_2} e^{-\beta(E_{\mathbf{k}_1}+E_{\mathbf{k}_2})}M_{\mathbf{x}_1,\mathbf{x}_2}|\langle \mathbf{k}_1\mathbf{k}_2|\mathbf{x}_1\mathbf{x}_2\rangle|^2, \end{aligned} \quad (32)$$

where we have inserted complete sets of states in coordinate space $\{|\mathbf{x}_1\mathbf{x}_2\rangle\}$ and in the basis $\{|\mathbf{k}_1\mathbf{k}_2\rangle\}$ of eigenstates of $\hat{H}_0$, whose single-particle eigenstates $|\mathbf{k}\rangle$ have eigenvalues $E_{\mathbf{k}}$. We have also made use of the fact that $\hat{V}_{int}$ is diagonal in coordinate space, such that

$$M_{\mathbf{x}_1,\mathbf{x}_2} = 1 + C\ell^{-d}\delta_{\mathbf{x}_1,\mathbf{x}_2}, \quad (33)$$

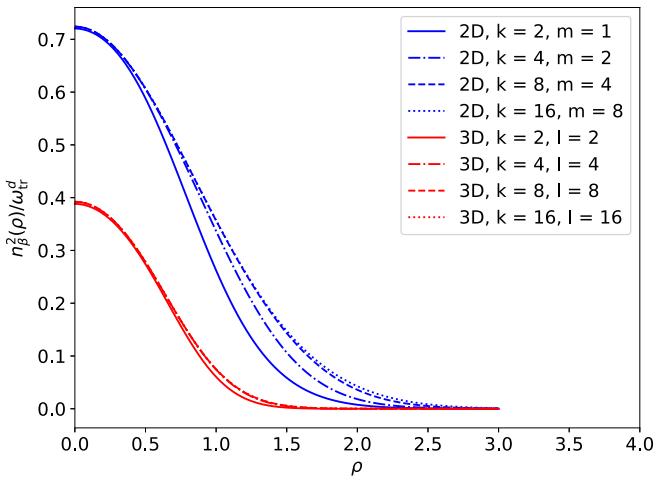

FIG. 1. $n_\beta^2(\mathbf{x})/\omega_{\rm tr}^d$ as a function of the radial coordinate ρ, for several cutoff values of the quantum numbers k, m in 2D (top four blue curves) and k, l in 3D (bottom four red curves); in the latter case, the quantum number m is summed over its full range $[-l, l]$. In this plot, $\omega_z/\omega_{\rm tr} = 1/2$.

where $C = \ell^d(e^{\beta g_d} - 1)$, and we have introduced a spatial lattice spacing ℓ as a regulator.

Thus,

$$\Delta Q_{1,1} = C \sum_{\mathbf{k}_1,\mathbf{k}_2,\mathbf{x}} \ell^d e^{-\beta(E_{\mathbf{k}_1}+E_{\mathbf{k}_2})} |\langle \mathbf{k}_1\mathbf{k}_2|\mathbf{x}\,\mathbf{x}\rangle|^2. \tag{34}$$

The computationally demanding part of this calculation is the overlap function $|\langle \mathbf{k}_1\mathbf{k}_2|\mathbf{x}\,\mathbf{x}\rangle|^2$. In this particular case, i.e., for $\Delta Q_{1,1}$, the overlap function can be factorized as $|\langle \mathbf{k}_1|\mathbf{x}\rangle|^2|\langle \mathbf{k}_2|\mathbf{x}\rangle|^2$. Upon summing over $\mathbf{k}_1, \mathbf{k}_2$, we obtain a simpler expression,

$$\Delta Q_{1,1} = C \sum_{\mathbf{x}} \ell^d n_\beta^2(\mathbf{x}), \tag{35}$$

where

$$n_\beta(\mathbf{x}) = \sum_{\mathbf{k}} e^{-\beta E_{\mathbf{k}}} |\langle \mathbf{k}|\mathbf{x}\rangle|^2, \tag{36}$$

which is the finite-temperature density profile of the system in the trapping potential. The exponential decay with the energy will enable us to cut off the sum over $\mathbf{k}$ without significantly losing precision. We show a representative example of such cutoff effects in Fig. 1.

Notice that $n_\beta(\mathbf{x})$ has units of $\omega_{\rm tr}^{d/2}$ [which corresponds to $(\text{length})^{-d}$] and it is a function of the dimensionless ratio $\rho = \omega_{\rm tr}^{1/2}\, r$ (see below for 2D and 3D examples), where $r = |\mathbf{x}|$. Upon taking the continuum limit,

$$\Delta Q_{1,1} \to \frac{C}{\lambda_T^d} \int d^d\bar{\mathbf{x}}\, (2\pi\beta\omega_{\rm tr})^{d/2} \frac{n_\beta^2(\bar{\mathbf{x}})}{\omega_{\rm tr}^d}, \tag{37}$$

where $\bar{\mathbf{x}} = \omega_{\rm tr}^{1/2}\, \mathbf{x}$ is dimensionless.

Thus, in 2D,

$$n_\beta(\mathbf{x}) = \omega_{\rm tr} \frac{e^{-\rho^2}}{2\pi} \sum_{k,m} e^{-\beta E_{km}} f_{km}^{\rm 2D}(\rho^2), \tag{38}$$

whose units come from the prefactor $\omega_{\rm tr}$ and, as expected from symmetry considerations, is only a function of the radial coordinate (concentric with the trapping potential). Here,

$$f_{km}^{\rm 2D}(\rho^2) \equiv \frac{2\,k!}{(k+|m|)!} \rho^{2|m|} \left[L_k^{|m|}(\rho^2)\right]^2. \tag{39}$$

Similarly, in 3D,

$$n_\beta(\mathbf{x}) = \omega_{\rm tr}^{3/2} \frac{e^{-\rho^2}}{\sqrt{4\pi}} \sum_{k,l,m} e^{-\beta E_{klm}} f_{kl}^{\rm 3D}(\rho^2) \left[P_l^m(\cos\theta)\right]^2, \tag{40}$$

where

$$f_{kl}^{\rm 3D}(\rho^2) \equiv \frac{2^{k+2l+3}\,k!}{(2k+2l+1)!!} \rho^{2l} \left[L_k^{l+1/2}(\rho^2)\right]^2. \tag{41}$$

Using the above results, together with Eq. (16) for Δb_2, we solve for the dimensionless quantity C/λ_T^d in terms of Δb_2:

$$\frac{C}{\lambda_T^d} = \Delta b_2 \frac{Q_1}{(2\pi\beta\omega_{\rm tr})^{d/2}} \left[\int d^d\bar{\mathbf{x}}\, \frac{n_\beta^2(\bar{\mathbf{x}})}{\omega_{\rm tr}^d}\right]^{-1}. \tag{42}$$

2. Three-body sector: $\Delta Q_{2,1}$ for fermions

Following the same steps outlined above, it is straightforward to show that

$$\Delta Q_{2,1} = \frac{C}{2} \sum_{\mathbf{k}_1\mathbf{k}_2\mathbf{k}_3} e^{-\beta(E_{\mathbf{k}_1}+E_{\mathbf{k}_2}+E_{\mathbf{k}_3})} \times \sum_{\mathbf{x}_1\mathbf{x}_2} |\langle \mathbf{x}_1\mathbf{x}_2\mathbf{x}_1|\mathbf{k}_1\mathbf{k}_2\mathbf{k}_3\rangle|^2. \tag{43}$$

The overlap can be simplified slightly by factoring across distinguishable species,

$$\langle \mathbf{x}_1\mathbf{x}_2\mathbf{x}_1|\mathbf{k}_1\mathbf{k}_2\mathbf{k}_3\rangle = \langle \mathbf{x}_1\mathbf{x}_2|\mathbf{k}_1\mathbf{k}_2\rangle \langle \mathbf{x}_1|\mathbf{k}_3\rangle, \tag{44}$$

where $\langle \mathbf{x}_1\mathbf{x}_2|\mathbf{k}_1\mathbf{k}_2\rangle$ is a Slater determinant of single-particle states,

$$\langle \mathbf{x}_1\mathbf{x}_2|\mathbf{k}_1\mathbf{k}_2\rangle = \langle \mathbf{x}_1|\mathbf{k}_1\rangle\langle \mathbf{x}_2|\mathbf{k}_2\rangle - \langle \mathbf{x}_2|\mathbf{k}_1\rangle\langle \mathbf{x}_1|\mathbf{k}_2\rangle. \tag{45}$$

As in the case of $\Delta Q_{1,1}$, we will sum over the energy eigenstates first, and then perform the spatial sum. To that end, it is useful to define

$$n_\beta^F(\mathbf{x}_1, \mathbf{x}_2) = n_\beta(\mathbf{x}_1) \sum_{\mathbf{k}_1\mathbf{k}_2} e^{-\beta(E_{\mathbf{k}_1}+E_{\mathbf{k}_2})} |\langle \mathbf{x}_1\mathbf{x}_2|\mathbf{k}_1\mathbf{k}_2\rangle|^2, \tag{46}$$

such that

$$\Delta Q_{2,1} = \frac{C}{2} \sum_{\mathbf{x}_1\mathbf{x}_2} n_\beta^F(\mathbf{x}_1, \mathbf{x}_2). \tag{47}$$

As in the case of $n_\beta(\mathbf{x})$, the exponential decay with the energy allows us to cut off the double sum in $n_\beta^F(\mathbf{x}_1, \mathbf{x}_2)$ without significantly affecting the precision of the whole calculation.

3. Three-body sector: $\Delta Q_{2,1}$ for bosons

The bosonic case differs from the fermionic case in that we must use a permanent rather than a Slater determinant. Thus,

$$n_\beta^B(\mathbf{x}_1, \mathbf{x}_2) = n_\beta(\mathbf{x}_1) \sum_{\mathbf{k}_1\mathbf{k}_2} e^{-\beta(E_{\mathbf{k}_1}+E_{\mathbf{k}_2})} |\langle \mathbf{x}_1\mathbf{x}_2|\mathbf{k}_1\mathbf{k}_2\rangle|^2, \tag{48}$$

where the two-body overlap is now symmetric in its arguments, as befits bosons,

$$\langle \mathbf{x}_1\mathbf{x}_2|\mathbf{k}_1\mathbf{k}_2\rangle = \langle \mathbf{x}_1|\mathbf{k}_1\rangle\langle \mathbf{x}_2|\mathbf{k}_2\rangle + \langle \mathbf{x}_2|\mathbf{k}_1\rangle\langle \mathbf{x}_1|\mathbf{k}_2\rangle. \tag{49}$$

4. Gaussian quadrature

As shown above, the single-particle wave functions [cf. Eqs. (20) and (26)] and the associated density functions $n_\beta(\mathbf{x})$, $n_\beta^{F,B}(\mathbf{x}_1,\mathbf{x}_2)$, are governed in the radial variable by a Gaussian decay. For that reason, it is appropriate to calculate the corresponding integrals using the Gauss-Hermite quadrature. The corresponding M points x_i and M weights w_i allow us to estimate integrals according to

$$\int_{-\infty}^{\infty} dx\, e^{-x^2} f(x) = \sum_{i=0}^{M-1} w_i f(x_i). \tag{50}$$

In this work, we use the same quadrature points and weights as in our previous work of Refs. [33–35].

III. RESULTS

A. Noninteracting virial coefficients at finite angular momentum

For future reference and because we have not been able to locate these results elsewhere in the literature, we present here the calculation of the noninteracting virial expansion when $\omega_z \neq 0$. We begin with the well-known result for the partition function of spin-1/2 fermions in terms of the single-particle energies E:

$$\ln \mathcal{Z} = 2\sum_E \ln(1 + ze^{-\beta E}), \tag{51}$$

which is valid for arbitrary positive z, whereas for (doubly degenerate) bosons,

$$\ln \mathcal{Z} = 2\sum_E \ln\left(\frac{1}{1 - ze^{-\beta E}}\right), \tag{52}$$

which is valid for arbitrary $z < \exp(\beta E_0)$, where E_0 is the ground-state energy [$z = \exp(\beta E_0)$ being the well-known limit of Bose-Einstein condensation]. From these expressions, it is easy to see that the virial coefficients b_n for noninteracting bosons and fermions differ by a factor of $(-1)^{n+1}$. As is well known, for homogeneous, nonrelativistic fermions in d dimensions, $b_n = (-1)^{n+1} n^{-(d+2)/2}$. Below, we address the generalization of this formula to harmonically trapped systems at finite angular momentum in 2D and 3D.

1. Two spatial dimensions

In 2D, $E = E_{km} = \omega_{\rm tr}(2k + |m| + 1) + \omega_z m$, where $k \geqslant 0$ and m is summed over all integers. Thus, we may write the sum by Taylor expanding the logarithm as

$$\ln \mathcal{Z} = 2\sum_{n=1}^{\infty} \frac{(-1)^{n+1}}{n} z^n e^{-n\beta\omega_{\rm tr}} \sum_{k=0}^{\infty} e^{-\beta\omega_{\rm tr} 2kn} \times \left[\sum_{m=0}^{\infty} e^{-\beta\omega_+ mn} + \sum_{\bar{m}=1}^{\infty} e^{-\beta\omega_- \bar{m}n}\right], \tag{53}$$

where $\omega_\pm = \omega_{\rm tr} \pm \omega_z$. Carrying out the sums over k, m, $\bar{m}$, we obtain

$$\ln \mathcal{Z} = Q_1 \sum_{n=1}^{\infty} b_n z^n, \tag{54}$$

where

$$Q_1 b_n = \frac{2\,(-1)^{n+1}}{n} \frac{e^{-n\beta\omega_{\rm tr}}}{(1 - e^{-n\beta\omega_+})(1 - e^{-n\beta\omega_-})}. \tag{55}$$

Finally, to determine b_n, we use Q_1 as derived above in Eqs. (25) and (30), such that

$$b_n = \frac{(-1)^{n+1}}{n} e^{-\beta\omega_{\rm tr}(n-1)} \frac{(1-e^{-\beta\omega_+})(1-e^{-\beta\omega_-})}{(1-e^{-n\beta\omega_+})(1-e^{-n\beta\omega_-})}. \tag{56}$$

Note that the b_n are always finite, in particular in the "deconfinement limit" referred to in Sec. I, where $\omega_- \to 0$,

$$b_n \to b_n^{\rm DL2D} \equiv \frac{(-1)^{n+1}}{n^2} e^{-\beta\omega_{\rm tr}(n-1)} \frac{(1 - e^{-2\beta\omega_{\rm tr}})}{(1 - e^{-2n\beta\omega_{\rm tr}})}. \tag{57}$$

On the other hand, Q_1 diverges in that limit because the energy spectrum then becomes independent from m. Simply put, in that limit, the centrifugal motion due to rotation is strong enough to overcome the trapping potential and the system escapes to infinity. In terms of $\ln \mathcal{Z}$, the divergence may be regarded as a phase transition at $\omega_z = \omega_{\rm tr}$. Below we further interpret this limit, considering the 2D and 3D cases simultaneously.

We can now derive a virial expansion for the angular momentum and the z component of the moment of inertia,

$$\langle \hat{L}_z \rangle = \frac{\partial \ln \mathcal{Z}}{\partial(\beta\omega_z)} = Q_1 \sum_{n=1}^{\infty} L_n z^n, \tag{58}$$

where

$$L_n = \frac{1}{Q_1}\frac{\partial(Q_1 b_n)}{\partial(\beta\omega_z)} = n b_n \frac{e^{-n\beta\omega_-} - e^{-n\beta\omega_+}}{(1 - e^{-n\beta\omega_+})(1 - e^{-n\beta\omega_-})} \tag{59}$$

and

$$I_z = \frac{\partial^2 \ln \mathcal{Z}}{\partial(\beta\omega_z)^2} = Q_1 \sum_{n=1}^{\infty} I_n z^n, \tag{60}$$

where

$$I_n = \frac{1}{Q_1}\frac{\partial(Q_1 L_n)}{\partial(\beta\omega_z)} = -nL_n\left[\frac{e^{-n\beta\omega_+} + e^{-n\beta\omega_-}}{e^{-n\beta\omega_+} - e^{-n\beta\omega_-}} + \frac{2(e^{-n\beta\omega_+} - e^{-n\beta\omega_-})}{(1 - e^{-n\beta\omega_+})(1 - e^{-n\beta\omega_-})}\right]. \tag{61}$$

Note that correctly, $L_n \to 0$ at $\omega_+ = \omega_-$, which corresponds to $\omega_z = 0$, i.e., no rotation. On the other hand, as may be expected from our previous discussion, $L_n \to \infty$ as $\omega_- \to 0$, as in that limit the induced rotation overpowers the external potential that holds the system together. Furthermore, at $\omega_z = 0$, a finite moment of inertia remains,

$$I_n \to 2n(-1)^{n+1} e^{-(2n-1)\beta\omega_{\rm tr}} \frac{(1 - e^{-\beta\omega_{\rm tr}})^2}{(1 - e^{-n\beta\omega_{\rm tr}})^4}, \tag{62}$$

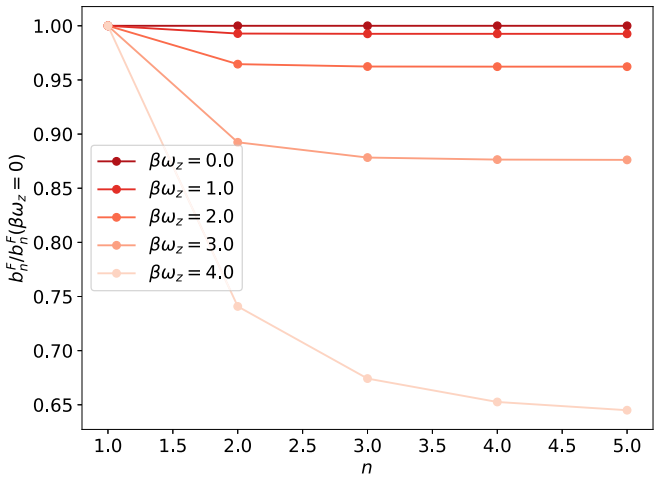

FIG. 2. Noninteracting b_n normalized by their nonrotating, noninteracting values $b_n(\beta\omega_z = 0)$, as functions of n for a few values of $\beta\omega_z$ and fixed $\beta\omega_{\rm tr} = 5$. The ratio $b_n/b_n(\beta\omega_z = 0)$ is the same for bosons and fermions, and is the same in 2D and 3D.

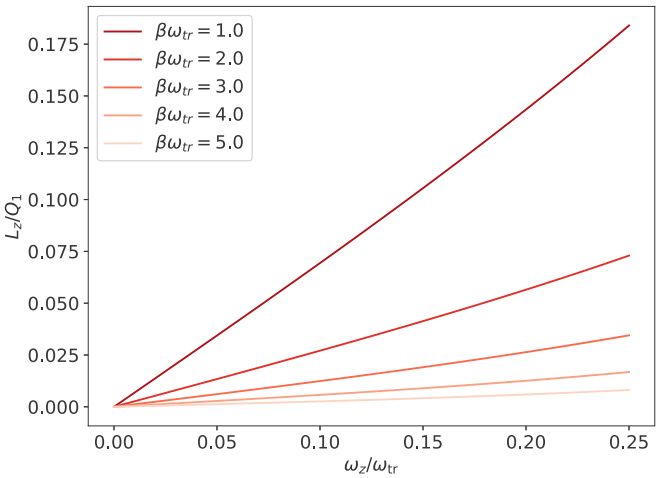

FIG. 3. Noninteracting L_z/Q_1 for bosons in 3D, as a function of $\omega_z/\omega_{\rm tr}$ for a few different temperatures $\beta\omega_{\rm tr}$, at third order in the virial expansion.

which characterizes the static response to small rotation frequencies within the virial expansion, as a function of $\beta\omega_{\rm tr}$.

2. *Three spatial dimensions*

In 3D, $E = E_{klm} = \omega_{\rm tr}(2k + l + 3/2) + \omega_z m$, where $k \geqslant 0$, $l \geqslant 0$, and $-l \leqslant m \leqslant l$. Therefore, analyzing the problem as in the 2D case, we obtain

$$Q_1 b_n = \frac{2(-1)^{n+1}}{n} \frac{e^{-\frac{3}{2}n\beta\omega_{\rm tr}}}{(1-e^{-n\beta\omega_{\rm tr}})(1-e^{-n\beta\omega_+})(1-e^{-n\beta\omega_-})} \tag{63}$$

and

$$b_n = \frac{(-1)^{n+1}}{n} e^{-\frac{3}{2}\beta\omega_{\rm tr}(n-1)} \times \frac{(1-e^{-\beta\omega_{\rm tr}})(1-e^{-\beta\omega_+})(1-e^{-\beta\omega_-})}{(1-e^{-n\beta\omega_{\rm tr}})(1-e^{-n\beta\omega_+})(1-e^{-n\beta\omega_-})}. \tag{64}$$

As in the 2D case, the b_n are always finite and, in particular in the deconfinement limit $\omega_- \to 0$,

$$b_n \to b_n^{\rm DL3D} \equiv \frac{(-1)^{n+1}}{n^2} e^{-\frac{3}{2}\beta\omega_{\rm tr}(n-1)} \times \frac{(1-e^{-\beta\omega_{\rm tr}})}{(1-e^{-n\beta\omega_{\rm tr}})} \frac{(1-e^{-2\beta\omega_{\rm tr}})}{(1-e^{-2n\beta\omega_{\rm tr}})}, \tag{65}$$

whereas Q_1 diverges in that limit. In this case, the problem can be traced back to the infinite sequence of states for which $\ell = -m$. We can also obtain expressions for the virial expansion of the angular momentum and the moment of inertia. Because the dependence of $Q_1 b_n$ on ω_+ and ω_- is the same in 2D and 3D, the relationship between L_n and b_n is identical in 2D and 3D, i.e., Eq. (59) is valid in 3D, as long as the b_n corresponding to 3D is used in the right-hand side. Similarly, Eq. (61) for I_n carries over to 3D, as long as the L_n corresponding to 3D is used in the right-hand side. As expected, and as in the 2D case, $L_n \to 0$ at $\omega_z = 0$, whereas

$$I_n \to 2n(-1)^{n+1} e^{-\frac{1}{2}\beta\omega_{\rm tr}(5n-3)} \frac{(1-e^{-\beta\omega_{\rm tr}})^3}{(1-e^{-n\beta\omega_{\rm tr}})^5}. \tag{66}$$

The impact of rotation, i.e., a finite $\beta\omega_z$ on a noninteracting system, is displayed in Fig. 2, where we show the ratio of the rotating to nonrotating virial coefficients. This ratio is the same for bosons and fermions in the noninteracting case and it drastically increases as ω_z approaches $\omega_{\rm tr}$. At large n, this ratio becomes

$$\frac{b_n}{b_n(\beta\omega_z = 0)} \to \frac{(1-e^{-\beta\omega_+})(1-e^{-\beta\omega_-})}{(1-e^{-\beta\omega_{\rm tr}})^2}. \tag{67}$$

Naturally, the total angular momentum will increase with ω_z. For a noninteracting system, the result is shown in Fig. 3 as a function of $\omega_z/\omega_{\rm tr}$, at several temperatures $\beta\omega_{\rm tr}$. At small ω_z, we find the linear response regime from which we can extract the moment of inertia I_z, as shown in Fig. 4. At the lowest temperatures (highest values of $\beta\omega_{\rm tr}$), the response of the system to rotation is highly suppressed, as seen in both Figs. 3 and 4. On the other hand, at high temperatures (low

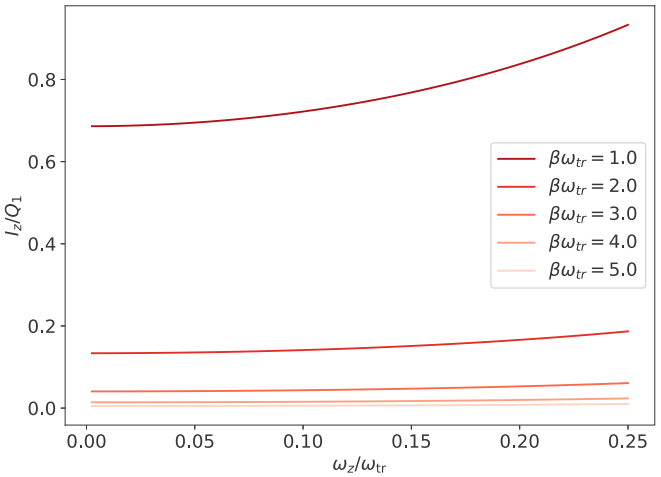

FIG. 4. Noninteracting I_z/Q_1 for bosons in 3D, as a function of $\omega_z/\omega_{\rm tr}$ for a few different temperatures $\beta\omega_{\rm tr}$, at third order in the virial expansion.

$\beta\omega_{\rm tr}$), where response is higher, we find a mild nonlinear regime in which I_z varies as a function of $\omega_z/\omega_{\rm tr}$.

3. The virial expansion in the deconfinement limit

Using the limiting expressions for the trapped, rotating b_n in 2D and 3D, namely, Eqs. (57) and (65), respectively, we may analyze the behavior of the system in that limit. To that end, we analyze those equations isolating their asymptotic form, which dominates the behavior of the virial expansion series,

$$b_n^{\rm DL2D} \simeq 2\frac{(-1)^{n+1}}{n^2}e^{-\beta\omega_{\rm tr}n}\sinh(\beta\omega_{\rm tr}), \tag{68}$$

$$b_n^{\rm DL3D} \simeq 4\frac{(-1)^{n+1}}{n^2}e^{-\frac{3}{2}\beta\omega_{\rm tr}n}\sinh(\beta\omega_{\rm tr}/2)\sinh(\beta\omega_{\rm tr}). \tag{69}$$

We thus see that the thermodynamics of the deconfined limit is governed in 2D by

$$\frac{\ln\mathcal{Z}}{Q_1} \simeq -2\sinh(\beta\omega_{\rm tr})\,{\rm Li}_2(-e^{-\beta\omega_{\rm tr}}z), \tag{70}$$

where ${\rm Li}_n(x)$ is the polylogarithm function of order n. Similarly, in 3D, we obtain

$$\frac{\ln\mathcal{Z}}{Q_1} \simeq -4\sinh(\beta\omega_{\rm tr}/2)\sinh(\beta\omega_{\rm tr})\,{\rm Li}_2\big(-e^{-\frac{3}{2}\beta\omega_{\rm tr}}z\big). \tag{71}$$

Notably, and prefactors aside, both the 2D and 3D cases are completely captured by the *same* polylogarithm function. More specifically, ${\rm Li}_2(x)$ is the same function that characterizes the 2D *homogeneous* quantum gas (both fermions and bosons). We therefore see explicitly how, in the deconfined limit, the maximized angular momentum flattens the (3D) system and effectively turns it into a homogeneous 2D gas, with a shifted chemical potential. While above we have written the results for fermions, analogous expressions are valid for bosons.

B. Interaction effects on the virial expansion

In this section we use our results for Δb_2 and Δb_3 to calculate the angular momentum equation of state, as well as the static response encoded in the moment of inertia. Denoting the noninteracting grand-canonical partition function by $\mathcal{Z}_0$, we have

$$\ln(\mathcal{Z}/\mathcal{Z}_0) = Q_1\sum_{n=2}^{\infty}\Delta b_n z^n, \tag{72}$$

such that the interaction effect on the angular momentum virial coefficient L_n is

$$\Delta L_n = \frac{1}{Q_1}\frac{\partial(Q_1\Delta b_n)}{\partial(\beta\omega_z)} = \frac{\partial(\Delta b_n)}{\partial(\beta\omega_z)} + \Delta b_n\frac{\partial(\ln Q_1)}{\partial(\beta\omega_z)}, \tag{73}$$

and its counterpart for the moment of inertia is

$$\Delta I_n = \frac{1}{Q_1}\frac{\partial(Q_1\Delta L_n)}{\partial(\beta\omega_z)} = \frac{\partial(\Delta L_n)}{\partial(\beta\omega_z)} + \Delta L_n\frac{\partial(\ln Q_1)}{\partial(\beta\omega_z)}, \tag{74}$$

where, using the previous equation for ΔL_n,

$$\frac{\partial(\Delta L_n)}{\partial(\beta\omega_z)} = \frac{\partial^2(\Delta b_n)}{\partial(\beta\omega_z)^2} + \frac{\partial(\Delta b_n)}{\partial(\beta\omega_z)}\frac{\partial(\ln Q_1)}{\partial(\beta\omega_z)} + \Delta b_n\frac{\partial^2(\ln Q_1)}{\partial(\beta\omega_z)^2}. \tag{75}$$

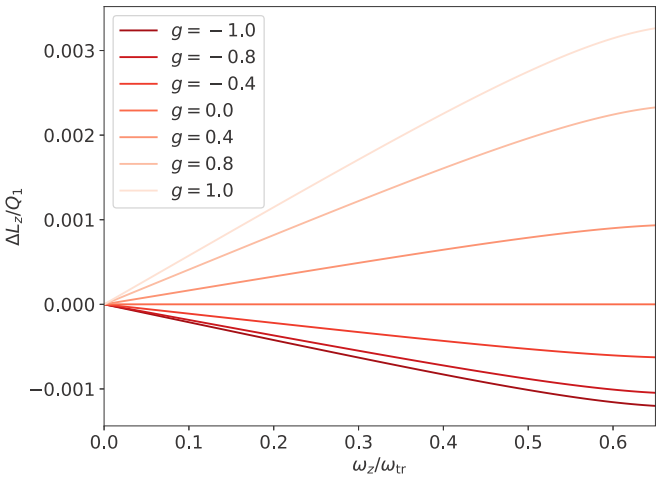

FIG. 5. Interaction-induced change in the angular momentum of a 3D Fermi gas with attractive and repulsive contact interactions, as a function of the rotation frequency ω_z in units of the trapping frequency $\omega_{\rm tr}$, at $z = \exp(-2.0)$.

Using the above formulas, along with the expressions obtained above for Δb_2 and Δb_3 in the coarse temporal lattice approximation, we readily obtain expressions for the interaction-induced change in the second- and third-order virial coefficients for the angular momentum and moment of inertia, namely, ΔL_2, ΔL_3, ΔI_2, and ΔI_3. Based on those, we can rebuild $\langle\hat{L}_z\rangle/Q_1$ and I_z/Q_1 and explore their change due to interactions in the virial region, which we show for fermions in Figs. 5 and 6. In both figures, we find that interactions change the response to rotation: both the angular momentum and the moment of inertia are modified by correlations, and the effect increases with ω_z. In particular, attractive interactions tend to make the system more compact (i.e., they reduce the size of the cloud), thus reducing the moment of inertia and the total angular momentum, for a given rotational

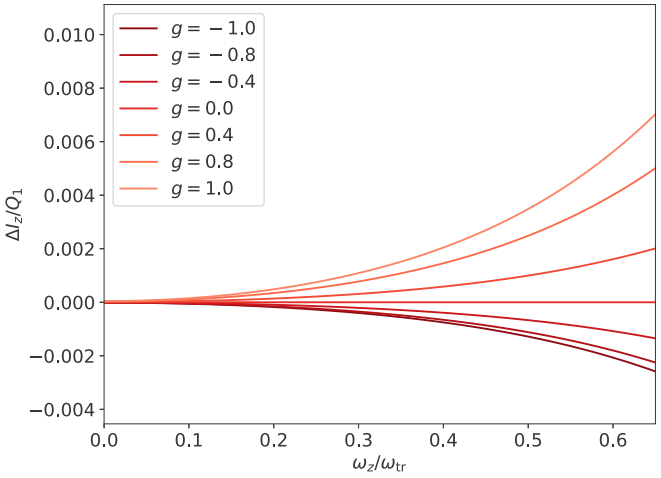

FIG. 6. Interaction-induced change in the moment of inertia of a 3D Fermi gas with attractive and repulsive contact interactions, as a function of the rotation frequency ω_z in units of the trapping frequency $\omega_{\rm tr}$, at $z = \exp(-2.0)$.

frequency. The corresponding opposite behavior is found for repulsive interactions.

IV. SUMMARY AND CONCLUSIONS

In this work, we have characterized the thermodynamics of rotating Bose and Fermi gases in 2D and 3D using the virial expansion. To that end, we calculated the effect of rotation on the virial coefficients b_n corresponding to the pressure and density equations of state, as well as on the virial coefficients for the angular momentum L_n and moment of inertia I_n. We carried out calculations for interacting as well as noninteracting systems.

In the absence of interactions, we obtained analytic formulas for b_n, L_n, and I_n in 2D and 3D, which were absent from the literature to the best of our knowledge. We noted that while the b_n remain finite when ω_z approaches $\omega_{\rm tr}$, the L_n, and I_n coefficients diverge, as does the single-particle partition function Q_1. The origin of the divergence is traced back to the fact that the system becomes unstable at $\omega_z = \omega_{\rm tr}$; in that deconfinement limit, the high angular velocity enables particles to escape the trapping potential. By exploring the asymptotic behavior of b_n in that limit, we found that (up to overall factors) it corresponds to that of a homogeneous 2D gas with a chemical potential shifted by the zero-point energy of the trapping potential.

To address the interacting cases, we implemented a coarse temporal lattice approximation, which allowed us to bypass solving the rotating n-body problem to calculate the nth-order virial coefficient, which we accessed at second and third orders. While calculations at such orders have been shown to capture at least part of the high-temperature thermodynamics of ultracold gases (see, e.g., Ref. [26]), it is a natural question of whether higher-order coefficients can be computed. In the proposed approximation, higher orders have been computed with and without a trapping potential [17–19,27,31,32], but at considerably higher computational cost, which will only increase when adding finite angular momentum. (Specifically, the computational scaling arises from nested sums that scale with the size of the single-particle basis, such that each new coefficient is exponentially more expensive to compute than its predecessor). On the other hand, we have shown that the noninteracting b_n are exponentially suppressed with n, with a characteristic decay set by $\beta\omega_{\rm tr}$, which likely persists once interactions are turned on, thus limiting the motivation to pursue higher-order virial coefficients for trapped systems.

Based on those results, we obtained qualitative estimates for the angular momentum as well as the moment of inertia, as functions of the angular velocity $0 < \omega_z < \omega_{\rm tr}$ and temperature $\beta\omega_{\rm tr}$. Notably, we find that both the interacting and noninteracting cases display linear response to rotation at low ω_z, as expected, but we are also able to distinguish a nonlinear regime in which I_z varies with ω_z; this is most evident at high temperatures and above $\omega_z/\omega_{\rm tr} \simeq 0.1$.

Our work represents a step toward characterizing the properties of rotating matter in high-temperature regimes. Future studies using increased computational power should be able to explore higher-order corrections to the coarse lattice approximation presented here.

ACKNOWLEDGMENTS

We would like to thank Jens Braun for useful comments on the manuscript. This material is based upon work supported by the National Science Foundation under Grant No. PHY1452635 (Computational Physics Program). C.E.B. acknowledges support from the US Department of Energy through the Computational Science Graduate Fellowship (DOE CSGF) under Grant No. DE-FG02-97ER25308.

APPENDIX: SINGLE-PARTICLE BASIS IN 2D

For completeness, in this Appendix we show the solution of the Schrödinger equation for a harmonically trapped particle coupled to the z component of angular momentum in 2D. The purpose of presenting this information is to establish our notation and to provide a reference point for future work.

We begin with the Schrödinger equation in polar coordinates,

$$\left(-\frac{\partial^2}{\partial r^2} - \frac{1}{r}\frac{\partial}{\partial r} - \frac{1}{r^2}\frac{\partial^2}{\partial \phi^2} + m^2\omega_{\rm tr}^2 r^2 - 2mE\right)\Psi(r,\phi) = 0.$$

We then change variables such that $\rho = m\sqrt{\omega_{\rm tr}}r$, and $m, \hbar = 1$, which yields

$$r \to \frac{1}{\sqrt{\omega_{\rm tr}}}\rho,$$
$$\frac{\partial}{\partial r} \to \sqrt{\omega_{\rm tr}}\frac{\partial}{\partial \rho},$$
$$\frac{\partial^2}{\partial r^2} \to \omega_{\rm tr}\frac{\partial^2}{\partial \rho^2}.$$

With those replacements, we write $\Psi(\rho,\phi)$ as a product of functions of two individual variables, $\Psi(\rho,\phi) = R(\rho)\Phi(\phi)$, such that

$$\left[-\left(\rho^2\frac{\partial^2}{\partial\rho^2} + \rho\frac{\partial}{\partial\rho} + \frac{\partial^2}{\partial\phi^2}\right) + \rho^4 - 2\rho^2\frac{E}{\omega_{\rm tr}}\right]R(\rho)\Phi(\phi) = 0.$$

This decouples our partial differential equation into two ordinary equations, each of which must be equal to a constant $\tilde{m}^2$,

$$-\frac{1}{\Phi(\phi)}\frac{\partial^2}{\partial\phi^2}\Phi(\phi) = \tilde{m}^2,$$
$$-\frac{\rho^2}{R(\rho)}\frac{\partial^2 R(\rho)}{\partial\rho^2} - \frac{\rho}{R(\rho)}\frac{\partial R(\rho)}{\partial\rho} + \rho^4 - 2\rho^2\frac{E}{\omega_{\rm tr}} = -\tilde{m}^2.$$

We can solve the equation for $\Phi(\phi)$ straightforwardly: $\Phi(\phi) \propto e^{i\tilde{m}\phi}$, with the constraint that $\tilde{m}$ must be an integer to ensure the solution is not multivalued.

The equation for ρ, setting $\tilde{E} = E/\omega_{\rm tr}$, is then

$$-\rho^2\frac{\partial^2 R(\rho)}{\partial\rho^2} - \rho\frac{\partial R(\rho)}{\partial\rho} + (\tilde{m}^2 + \rho^4 - 2\rho^2\tilde{E})R(\rho) = 0. \tag{A1}$$

At long distances ($\rho \to \infty$), we have a harmonic oscillator equation,

$$-\frac{\partial^2 R(\rho)}{\partial\rho^2} + \rho^2 R(\rho) = 2\tilde{E}R(\rho), \tag{A2}$$

which indicates that at long distances, the solution behaves as a Gaussian.

At short distances ($\rho \ll 1$), on the other hand, our equation reduces to

$$-\rho^2 \frac{\partial^2 R(\rho)}{\partial \rho^2} - \rho \frac{\partial R(\rho)}{\partial \rho} + \widetilde{m}^2 R(\rho) = 0. \tag{A3}$$

We can approach this by proposing proposing $R(\rho) = R_0 \rho^c$, which leads to an equation for the power c in terms of our constant $\widetilde{m}$,

$$-c^2 = \widetilde{m}^2, \; c = \pm \widetilde{m}. \tag{A4}$$

The case $\widetilde{m} = 0$ yields two solutions: a constant $R(\rho) = R_0$ and $R(\rho) = \ln \rho$. We can discard the second one since it diverges at the origin, which our wave function should not do. For the same reason, we discard the case $\widetilde{m} < 0$. Therefore, the short-distance behavior is $R(\rho) \propto \rho^{|\widetilde{m}|}$.

Based on the above analysis, we propose, for the full solution, the form

$$R(\rho) = e^{-\rho^2/2} \rho^{|\widetilde{m}|} F(\rho), \tag{A5}$$

where $F(\rho)$ is a function to be determined. This captures the behavior of $R(\rho)$ in our limiting cases. With that form, the radial equation becomes

$$\rho^2 \frac{\partial^2 F(\rho)}{\partial \rho^2} + \frac{\partial F(\rho)}{\partial \rho}(b_{\widetilde{m}} \rho - 2\rho^3) - 2 a_{\widetilde{m}} \rho^2 F(\rho) = 0, \tag{A6}$$

where $a_{\widetilde{m}} \equiv 1 - \widetilde{E} + |\widetilde{m}|$ and $b_{\widetilde{m}} \equiv 2|\widetilde{m}| + 1$. We propose a power series form,

$$F(\rho) = \sum_{k=0}^{\infty} \rho^k c_k, \tag{A7}$$

and obtain algebraic equations for c_k from Eq. (A6). Analyzing the lowest powers, we obtain the following conditions: From the lowest two powers of ρ, we find that c_0 is not fixed, but that $c_1 = 0$. The remaining coefficients are related by the recursion

$$c_{k+2} = \frac{2(k + a_{\widetilde{m}})}{(k+2)(k+1+b_{\widetilde{m}})} c_k. \tag{A8}$$

Thus, if both c_0 and c_1 vanish, then the solution vanishes identically. On the other hand, setting $c_0 = 1$, only the odd coefficients vanish and we obtain the remaining coefficients recursively. The overall normalization can be set after the fact since the equation is linear. The series terminates if $k = a_{\widetilde{m}}$ for some $k = 2n \geqslant 0$ (recall that only the even-k survive), which yields the quantization condition,

$$\frac{E}{\omega_{\mathrm{tr}}} = 2n + |\widetilde{m}| + 1. \tag{A9}$$

[1] S. Giorgini, L. P. Pitaevskii, and S. Stringari, Theory of ultracold Fermi gases, Rev. Mod. Phys. **80**, 1215 (2008).

[2] I. Bloch, J. Dalibard, and W. Zwerger, Many-body physics with ultracold gases, Rev. Mod. Phys. **80**, 885 (2008).

[3] M. Lewenstein, A. Sanpera, and V. Ahufinger, *Ultracold Atoms in Optical Lattices: Simulating Quantum Many-body Systems*, (Oxford University Press, New York, 2012).

[4] C. Chin, R. Grimm, P. Julienne, and E. Tiesinga, Feshbach resonances in ultracold gases, Rev. Mod. Phys. **82**, 1225 (2010).

[5] F. Chevy and C. Mora, Ultra-cold polarized Fermi gases, Rep. Prog. Phys. **73**, 112401 (2010).

[6] *Ultracold Fermi Gases*, in *Proceedings of the International School of Physics "Enrico Fermi", Course CLXIV*, edited by M. Inguscio, W. Ketterle, and C. Salomon (IOS Press, Amsterdam, 2008).

[7] M. H. Anderson, J. R. Ensher, M. R. Matthews, C. E. Wieman, and E. A. Cornell, Observation of Bose-Einstein condensation in a dilute atomic vapor, Science **269**, 198 (1995).

[8] K. B. Davis, M.-O. Mewes, M. R. Andrews, N. J. van Druten, D. S. Durfee, D. M. Kurn, and W. Ketterle, Bose-Einstein Condensation in a Gas of Sodium Atoms, Phys. Rev. Lett. **75**, 3969 (1995).

[9] C. A. Regal, M. Greiner, and D. S. Jin, Observation of Resonance Condensation of Fermionic Atom Pairs, Phys. Rev. Lett. **92**, 040403 (2004).

[10] M. W. Zwierlein, C. A. Stan, C. H. Schunck, S. M. F. Raupach, A. J. Kerman, and W. Ketterle, Condensation of Pairs of Fermionic Atoms near a Feshbach Resonance, Phys. Rev. Lett. **92**, 120403 (2004).

[11] M. R. Matthews, B. P. Anderson, P. C. Haljan, D. S. Hall, M. J. Holland, J. E. Williams, C. E. Wieman, and E. A. Cornell, Watching a Superfluid Untwist Itself: Recurrence of Rabi Oscillations in a Bose-Einstein Condensate, Phys. Rev. Lett. **83**, 3358 (1999).

[12] K. W. Madison, F. Chevy, W. Wohlleben, and J. Dalibard, Vortex Formation in a Stirred Bose-Einstein Condensate, Phys. Rev. Lett. **84**, 806 (2000).

[13] M. W. Zwierlein, J. R. Abo-Shaeer, A. Schirotzek, C. H. Schunck, and W. Ketterle, Vortices and superfluidity in a strongly interacting fermi gas, Nature (London) **435**, 1047 (2005).

[14] N. Cooper, Rapidly rotating atomic gases, Adv. Phys. **57**, 539 (2008).

[15] A. L. Fetter, Rotating trapped Bose-Einstein condensates, Rev. Mod. Phys. **81**, 647 (2009).

[16] S. Stringari, Phase Diagram of Quantized Vortices in a Trapped Bose-Einstein Condensed Gas, Phys. Rev. Lett. **82**, 4371 (1999).

[17] C. R. Shill and J. E. Drut, Virial coefficients of 1D and 2D Fermi gases by stochastic methods and a semiclassical lattice approximation, Phys. Rev. A **98**, 053615 (2018).

[18] Y. Hou, A. Czejdo, J. DeChant, C. R. Shill, and J. E. Drut, Leading-order semiclassical approximation to the first seven virial coefficients of spin-1/2 fermions across spatial dimensions, Phys. Rev. A **100**, 063627 (2019).

[19] K. J. Morrell, C. E. Berger, and J. E. Drut, Third- and fourth-order virial coefficients of harmonically trapped fermions in a semiclassical approximation, Phys. Rev. A **100**, 063626 (2019).
[20] B. C. Mulkerin, C. J. Bradly, H. M. Quiney, and A. M. Martin, Universality in rotating strongly interacting gases, Phys. Rev. A **85**, 053636 (2012).
[21] B. C. Mulkerin, C. J. Bradly, H. M. Quiney, and A. M. Martin, Universality and itinerant ferromagnetism in rotating strongly interacting Fermi gases, Phys. Rev. A **86**, 053631 (2012).
[22] B. Jeevanesan and S. Moroz, Thermodynamics of two-dimensional bosons in the lowest Landau level, arXiv:1910.07808.
[23] K. Bencheikh, J. Bartel, and P. Quentin, Semiclassical description of finite fermion systems at finite temperature in a generalised Routhian approach, Nucl. Phys. A **764**, 79 (2006).
[24] Y. Li, Rotating ideal Fermi gases under a harmonic potential, Physica B **481**, 38 (2016).
[25] Y. Li and Q. Gu, The particle flow oscillations of rotating noninteracting gases in a two-dimensional harmonic trap, Phys. Lett. A **380**, 353 (2016).
[26] X.-J. Liu, Virial expansion for a strongly correlated Fermi system and its application to ultracold atomic Fermi gases, Phys. Rep. **524**, 37 (2013).
[27] Y. Yan and D. Blume, Path-Integral Monte Carlo Determination of the Fourth-Order Virial Coefficient for a Unitary Two-Component Fermi Gas with Zero-Range Interactions, Phys. Rev. Lett. **116**, 230401 (2016).
[28] E. Beth and G. E. Uhlenbeck, The quantum theory of the non-ideal gas. II. Behaviour at low temperatures, Physica (Utrecht) **4**, 915 (1937).
[29] X. J. Liu, H. Hu, and P. D. Drummond, Exact few-body results for strongly correlated quantum gases in two dimensions, Phys. Rev. B **82**, 054524 (2010).
[30] T. Busch, B.-G. Englert, K. Rzażewski, and M. Wilkens, Found. Phys. **28**, 549 (1998).
[31] Y. Hou and J. E. Drut, The virial expansion of attractively interacting Fermi gases in 1D, 2D, and 3D, up to fifth order, arXiv:1908.00174.
[32] Y. Hou and J. E. Drut, The Fourth- and Fifth-order Virial Coefficients from Weak-coupling to Unitarity, Phys. Rev. Lett. **125**, 050403 (2020).
[33] C. E. Berger, E. R. Anderson, and J. E. Drut, Energy, contact, and density profiles of one-dimensional fermions in a harmonic trap via nonuniform-lattice Monte Carlo calculations, Phys. Rev. A **91**, 053618 (2015).
[34] C. E. Berger, J. E. Drut, and W. J. Porter, Hard-wall and non-uniform lattice Monte Carlo approaches to one-dimensional Fermi gases in a harmonic trap, Comput. Phys. Commun. **208**, 103 (2016).
[35] Z. Luo, C. E. Berger, and J. E. Drut, Harmonically trapped fermions in two dimensions: Ground-state energy and contact of SU(2) and SU(4) systems via a nonuniform lattice Monte Carlo method, Phys. Rev. A **93**, 033604 (2016).